

Binuclear Aroyl and Carbamoyl Complexes of Iron: X-ray Crystal Structures of $[\text{Fe}_2(\mu:\sigma,\sigma'\text{-OCR})_2(\text{CO})_5(\text{PPh}_3)]$ ($\text{R} = \text{C}_6\text{H}_3\text{Me}_{2-2,6}, \text{N}^i\text{Pr}_2$)

Stephen Anderson, Anthony F. Hill,*¹
Alexandra M. Z. Slawin, Andrew J. P. White, and
David J. Williams

Department of Chemistry, Imperial College of Science,
Technology and Medicine, South Kensington,
London SW7 2AY, United Kingdom

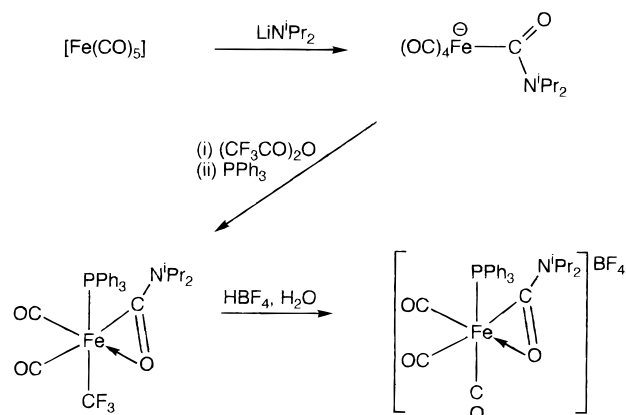
Received June 6, 1997

Introduction

We have recently shown² in an attempt to synthesize aminomethylidyne complexes of iron that sequential treatment of $[\text{Fe}(\text{CO})_5]$ with lithium diisopropylamide (LiN^iPr_2), trifluoroacetic anhydride, and triphenylphosphine provides the trifluoromethyl–carbamoyl complex $[\text{Fe}(\eta^2\text{-OCN}^i\text{Pr}_2)(\text{CF}_3)(\text{CO})_2(\text{PPh}_3)]$ (Scheme 1), rather than the desired compound $[\text{Fe}(\equiv\text{CN}^i\text{Pr}_2)(\text{O}_2\text{CCF}_3)(\text{CO})_2(\text{PPh}_3)]$ which might have been anticipated by analogy with the corresponding group 6 chemistry.³ The failure of this strategy for group 8 metals can be traced to the the ambident nature of the nucleophilic acyl metallate involved: The complexes $[\text{Cr}\{\text{=C}(\text{OLi})\text{N}^i\text{Pr}_2\}(\text{CO})_5]$ and $[\text{Fe}\{\text{=C}(\text{OLi})\text{N}^i\text{Pr}_2\}(\text{CO})_4]$ differ in metal d-occupancy (d^6 vs d^8) and coordination number (6 vs 5), both factors which favor electrophilic attack at the metal center for group 8 complexes and at the acyl oxygen for group 6 complexes. The regioselectivity of electrophilic attack upon acyl tetracarbonyl ferrates has been addressed by Semmelhack⁴ and provides the basis for the synthetic utility of Collman's reagent.⁵ In one of the earliest investigations of the reactions of acylferrates with electrophiles, Fischer showed that treating $[\text{Fe}\{\text{=C}(\text{OLi})\text{Ph}\}(\text{CO})_4]$ with Brønsted acids leads to the formation of the bimetallic complex $[\text{Fe}_2(\mu:\sigma,\sigma'\text{-OCPH})_2(\text{CO})_6]$, which, by virtue of the unsymmetric benzoyl bridging, has chemically distinct iron centers.⁶

In our pursuit of alkylidyne complexes of iron, we have now turned our attention to the possibility of employing steric shielding to facilitate the possible formation and/or stabilization of an alkylidyne iron complex. Alkylidyne complexes of group 6 metals bearing the 2,6-dimethylphenyl substituent show considerably increased stability, relative to those of related

Scheme 1



benzylidyne complexes.⁷ Nevertheless, we find once again that an alkylidyne complex of iron is not the product of such a strategy. We report herein (i) the synthesis of the bis(μ -aroyl) bimetallic complex $[\text{Fe}_2(\mu:\sigma,\sigma'\text{-OCC}_6\text{H}_3\text{Me}_{2-2,6})_2(\text{CO})_5(\text{PPh}_3)]$ (**1**); (ii) the preparation of the related bis(carbamoyl) analogue $[\text{Fe}_2(\mu:\sigma,\sigma'\text{-OCN}^i\text{Pr}_2)_2(\text{CO})_5(\text{PPh}_3)]$ (**2**) via a number of complementary routes; and (iii) the comparative structural characterization of the complexes **1** and **2**, which represent variations on Fischer's original complex $[\text{Fe}_2(\mu:\sigma,\sigma'\text{-OCPH})_2(\text{CO})_6]$.⁶

Results and Discussion

The successive treatment of $[\text{Fe}(\text{CO})_5]$ with LiR ($\text{R} = \text{CH}_3, ^i\text{Bu}, ^t\text{Bu}, \text{C}_6\text{H}_4\text{OMe-4}$), $(\text{CF}_3\text{CO})_2\text{O}$, and PPh_3 leads to the formation of $[\text{Fe}(\text{CO})_3(\text{PPh}_3)_2]$ in high yield as effectively the only organometallic product. Although somewhat unfortunate for our purposes, this route is now the most convenient available for large-scale preparations of this complex. If, however, the more sterically congested $\text{LiC}_6\text{H}_3\text{Me}_{2-2,6}$ is employed, in addition to $[\text{Fe}(\text{CO})_3(\text{PPh}_3)_2]$ (*ca.* 30%) a second product is obtained which is formulated as the binuclear compound $[\text{Fe}_2(\mu:\sigma,\sigma'\text{-OCC}_6\text{H}_3\text{Me}_{2-2,6})_2(\text{CO})_5(\text{PPh}_3)]$ (**1**) (Scheme 2) on the basis of spectroscopic data and a single-crystal X-ray diffraction study (Tables 1 and 2, Figure 1, *vide infra*). The infrared data are not particularly diagnostic, but include an absorption at 1681 cm^{-1} , which is tentatively assigned to the bridging acyl group. Similarly, ^1H NMR data serve only to confirm that the four methyl groups of the aroyl bridges are chemically equivalent on the ^1H NMR time scale. The ^{13}C NMR data include a low-field resonance at 295.7 ppm which is due to the bridging aroyl carbonyl, in addition to three terminal carbonyl resonances. No molecular ion is observed in the FAB mass spectrum; however, peaks attributable to loss of one and five carbonyl ligands are readily identifiable. These data fail to unequivocally define the nature of the complex but are consistent with the solid-state structure revealed by crystallography and discussed below.

We have also prepared and structurally characterized (Tables 1 and 3, Figure 2) the bis(carbamoyl) complex $[\text{Fe}_2(\mu:\sigma,\sigma'\text{-OCN}^i\text{Pr}_2)_2(\text{CO})_5(\text{PPh}_3)]$ (**2**) which has a similar " $\text{Fe}_2\text{C}_2\text{O}_2$ " structural

(1) E-mail: a.hill@ic.ac.uk.

(2) (a) Anderson, S.; Hill, A. F.; Clark, G. R. *Organometallics*, **1992**, *11*, 1988. (b) Anderson, S.; Hill, A. F. *Organometallics* **1995**, *14*, 1562.

(3) (a) Anderson, S.; Hill, A. F. *J. Organomet. Chem.* **1990**, *394*, C24. (b) For a general review of alkylidyne chemistry see: Mayr, A.; Hoffmeister, H. *Adv. Organomet. Chem.* **1991**, *32*, 227.

(4) (a) Semmelhack, M. F.; Tamura, R. J. *J. Am. Chem. Soc.* **1983**, *105*, 4099. (b) For a discussion of alkylidyne complexes obtained by *O*-alkylation of acyl ferrates see: Kerber, R. C. In *Comprehensive Organometallic Chemistry II*; Abel, E. W., Stone, F. G. A., Wilkinson, G., Eds.; Pergamon: Oxford, 1995; Vol. 7.

(5) Collman, J. P. *Acc. Chem. Res.* **1975**, *8*, 342.

(6) (a) Fischer, E. O.; Kiener, V.; Bunbury, D. St. P.; Frank, E.; Lidley, P. F.; Mills, O. S. *J. Chem. Soc., Chem. Commun.* **1968**, 1378. (b) Fischer, E. O.; Kiener, V. *J. Organomet. Chem.* **1970**, *23*, 215. (c) Lidley, P. F.; Mills, O. S. *J. Chem. Soc. A* **1969**, 1279.

(7) (a) Dossett, S. J.; Hill, A. F.; Jeffery, J. C.; Marken, F.; Sherwood, P.; Stone, F. G. A. *J. Chem. Soc., Dalton Trans.* **1988**, 2453. (b) Hill, A. F.; Marken, F.; Nasir, B. A.; Stone, F. G. A. *J. Organomet. Chem.* **1989**, *363*, 311. (c) Dossett, S. J.; Hill, A. F.; Howard, J. A. K.; Nasir, B. A.; Spaniol, T. P.; Sherwood, P.; Stone, F. G. A. *J. Chem. Soc., Dalton Trans.* **1989**, 1871. (d) Anderson, S.; Hill, A. F.; Nasir, B. A. *Organometallics* **1995**, *14*, 2987.

Scheme 2

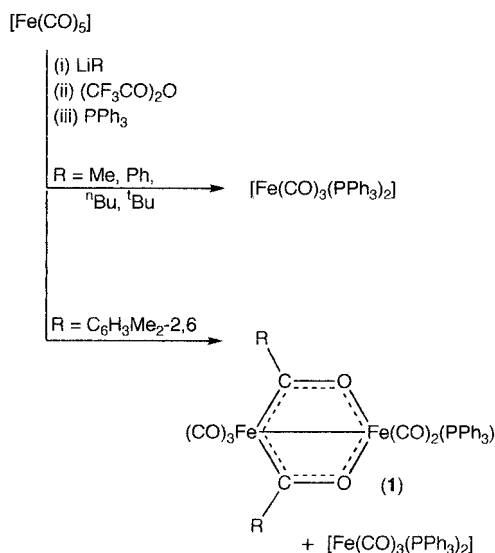


Table 1. Crystallographic Data for 1 and 2

	(1)	(2)
empirical formula	C ₄₁ H ₃₃ Fe ₂ O ₇ P	C ₃₇ H ₄₃ Fe ₂ N ₂ O ₇ P
fw	780.3	770.4
crystal system	monoclinic	monoclinic
space group	<i>P</i> 2 ₁ / <i>a</i>	<i>P</i> 2 ₁ / <i>n</i>
<i>a</i> (Å)	11.749(2)	12.398(2)
<i>b</i> (Å)	24.008(3)	16.050(4)
<i>c</i> (Å)	12.865(2)	20.145(4)
β (deg)	92.95(2)	106.74(2)
<i>V</i> (Å ³)	3624.1(9)	3838.9(13)
<i>Z</i>	4	4
<i>F</i> (000)	1608	1608
<i>T</i> (K)	293	293
λ (Å)	0.710 73	0.710 73
μ(Mo Kα) (mm ⁻¹)	0.895	0.845
ρ _{calc} (g cm ⁻³)	1.430	1.333
residuals		
<i>R</i> ^a	0.062	0.044
<i>R</i> _w ^b	0.059	0.046
e density (e Å ⁻³)		
max	0.62	0.37
min	-0.58	-0.51

^a $R = \sum ||F_o| - |F_c|| / \sum |F_o|$, ^b $R_w = \sum [(|F_o| - |F_c|)w^{1/2}] / \sum [|F_o|w^{1/2}]$, $w^{-1} = [\sigma(F) + 0.000 70F^2]$.

Table 2. Selected Bond Lengths (Å) and Angles (deg) for 1

bond lengths		interbond angles	
Fe(1)–Fe(2)	2.590(1)	Fe(1)–Fe(2)–P(2)	159.2(1)
Fe(1)–C(11)	1.803(7)	C(14)–Fe(1)–C(15)	85.8(2)
Fe(1)–C(12)	1.801(7)	O(14)–Fe(2)–O(15)	85.1(2)
Fe(1)–C(13)	1.799(7)	Fe(2)–Fe(1)–C(12)	160.7(2)
Fe(1)–C(14)	1.988(6)	Fe(1)–C(14)–O(14)	112.8(4)
Fe(1)–C(15)	1.954(5)	Fe(1)–C(15)–O(15)	115.1(4)
Fe(2)–O(14)	1.966(4)	C(14)–O(14)–Fe(2)	107.0(3)
Fe(2)–O(15)	1.996(4)	C(15)–O(15)–Fe(2)	104.5(3)
Fe(2)–C(21)	1.768(6)		
Fe(2)–C(22)	1.765(7)		
Fe(2)–P(2)	2.327(2)		
C(14)–O(14)	1.243(6)		
C(15)–O(15)	1.245(6)		

motif. This bimetallic complex results from a number of reactions, some strategic and some surprising. These are summarized in Scheme 3 and include (i) Li[Fe{C(=O)NⁱPr₂}(CO)₄] with mercuric chloride and triphenylphosphine; (ii) [Fe(η²-OCNⁱPr₂)(CO)₃(PPh₃)]BF₄ with diisopropylamine, (iii) [Fe(η²-OCNⁱPr₂)(CO)₂(PPh₃)] with K[HB(pz)₃] (pz = pyrazol-1-yl),

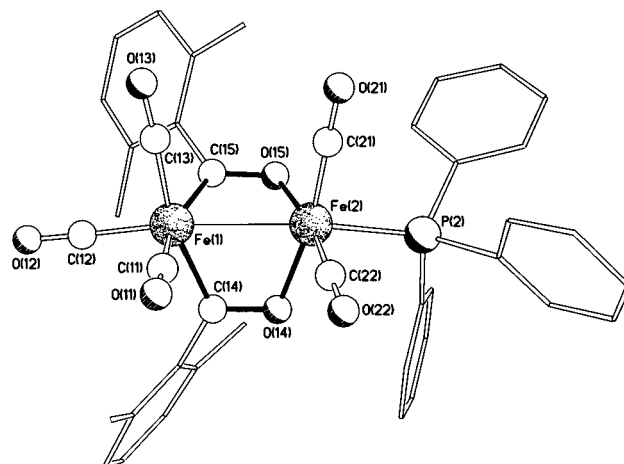


Figure 1. Molecular geometry for 1 (aryl groups simplified).

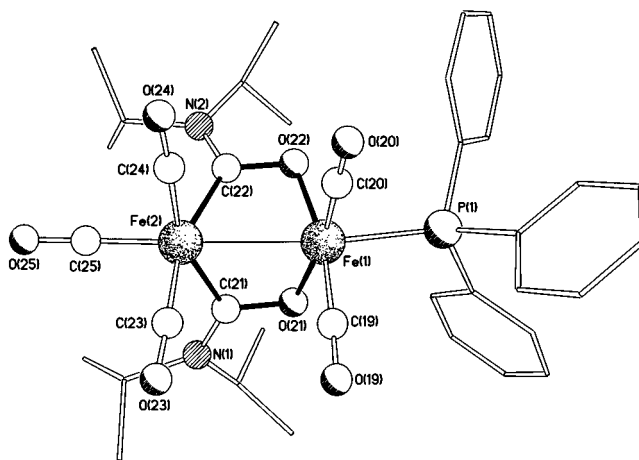


Figure 2. Molecular geometry of 2 (amino and phenyl groups simplified).

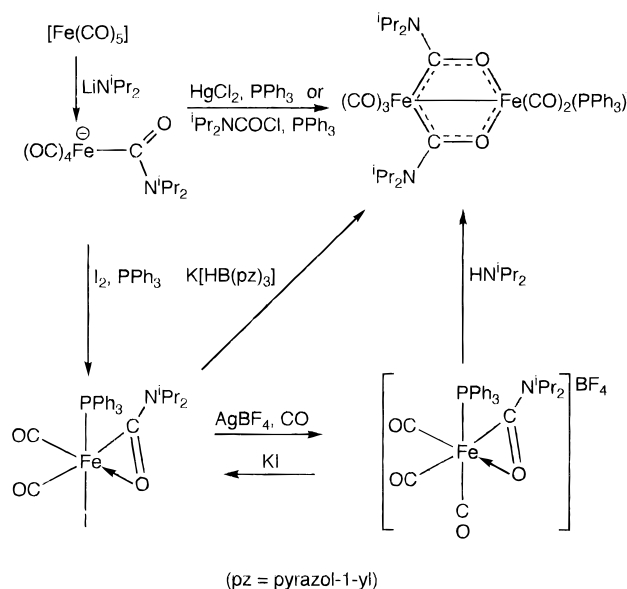
Table 3. Selected Bond Lengths (Å) and Angles (deg) for 2

bond lengths		interbond angles	
Fe(1)–Fe(2)	2.569(1)	Fe(2)–Fe(1)–P(1)	162.8(1)
Fe(1)–P(1)	2.320(1)	Fe(1)–Fe(2)–C(25)	169.9(1)
Fe(1)–O(21)	1.977(2)	O(21)–Fe(1)–O(22)	84.0(1)
Fe(1)–O(22)	1.956(2)	C(21)–Fe(2)–C(22)	82.8(1)
Fe(2)–C(21)	1.993(3)	Fe(2)–C(21)–O(21)	112.4(2)
Fe(2)–C(22)	2.013(3)	Fe(2)–C(22)–O(22)	112.1(2)
C(21)–O(21)	1.274(4)	C(21)–O(21)–Fe(1)	104.9(2)
C(22)–O(22)	1.270(4)	C(22)–O(22)–Fe(1)	105.8(2)
Fe(1)–C(19)	1.762(3)		
Fe(1)–C(20)	1.749(3)		
Fe(2)–C(23)	1.788(3)		
Fe(2)–C(24)	1.789(3)		
Fe(2)–C(25)	1.782(4)		
N(1)–C(21)	1.349(3)		
N(2)–C(22)	1.341(4)		

and (iv) Li[Fe{C(=O)NⁱPr₂}(CO)₄] with *N,N*-diisopropylcarbamoyl chloride and triphenylphosphine. The first of these methods provides the highest yields of 2. Clearly the formation of complex 2 is favored in a range of situations. Surprisingly, however, 2 cannot be detected as a side product of the synthesis of [Fe(η²-OCNⁱPr₂)(CF₃)(CO)₂(PPh₃)] from Li[Fe{C(=O)NⁱPr₂}(CO)₄], (CF₃CO)₂O, and PPh₃. This marked contrast to the synthesis of 1 indicates that the carbamoyl/acyl analogy has both utility and limitations.

The spectroscopic data for the two superficially isostructural complexes are quite different. Although carbonyl-associated infrared data are essentially comparable, the ¹H and ¹³C NMR

Scheme 3



data suggest that on the NMR time scale, **1** undergoes a dynamic process apparently involving rotation of the aryl group. The corresponding data for **2** indicate that the C–NⁱPr₂ groups are rigid. Thus four doublet resonances are observed for the methyl substituents in both the ¹H and ¹³C NMR spectra. Most conspicuously, however, the ¹³C resonance for the bridging carbamoyl carbon in **2** is moved to higher field relative to that for **1** and is not unequivocally differentiated from those due to the carbonyl ligands. Furthermore, the improved resolution resulting from a static structure allows the observation of ¹³C–³¹P couplings for these resonances. The lack of free rotation about the carbamoyl N–CO bond in **2** is a feature of carboxamido ligands which bridge the edges of triosmium and trirhenium clusters in the μ:σ(C),σ(O) mode.⁸ Such M(μ-OCNR₂)M bridges, once formed, appear to impart considerable stability on the clusters they support. The apparent discrepancy in data between the complexes **1** and **2** is presumably due to an enhanced carbene character for the acyl carbon atoms in **1** and similar low-field resonances are observed for the related hydrocarbyl substituted monoacyl(μ-thiolate) complexes prepared by Seyferth *et al.*⁹ The complex [Os₃(μ-OCPh)₂(CO)₁₀]¹⁰ shows a similarly low-field shift for the acyl bridge carbon (271.9 ppm), while related triosmium carboxamide complexes have resonances in the same region as for terminal carbonyl ligands.⁸ It should perhaps be noted that in these cluster compounds, it is not necessary (on EAN grounds at least) to invoke a metal–metal bond as part of the bridge motif. This is, however, a requirement for **1** and **2**.

- (8) (a) Kampe, C. E.; Kaesz, H. D. *Inorg. Chem.* **1984**, *23*, 4646. (b) Mayr, A.; Lin, Y. C.; Boag, N. M.; Kampe, C. E.; Knobler, C. B.; Kaesz, H. D. *Inorg. Chem.* **1984**, *23*, 4640. (c) Mayr, A.; Lin, Y. C.; Boag, N. M.; Kaesz, H. D. *Inorg. Chem.* **1982**, *21*, 1704. (d) Xue, Z. L.; Sieber, W. J.; Knobler, C. B.; Kaesz, H. D. *J. Am. Chem. Soc.* **1990**, *112*, 1825. (e) Jensen, C. M.; Chen, Y. J.; Kaesz, H. D. *J. Am. Chem. Soc.* **1984**, *106*, 4046. (f) Lin, Y. C.; Knobler, C. B.; Kaesz, H. D. *J. Am. Chem. Soc.* **1981**, *103*, 1216. (g) Kampe, C. E.; Boag, N. M.; Kaesz, H. D. *J. Mol. Catal.* **1983**, *21*, 297.
- (9) (a) A range of monoacyl bridged diiron complexes [Fe₂(μ:σ,σ'-OCR')(μ-SR)(CO)₇] have been shown to result from the reaction of [Fe₂(μ-SR)(CO)₈][−] with organomercuric halides [R'HgX]: Seyferth, D.; Archer, C. M.; Ruschke, D. P.; Cowie, M.; Hiltz, R. W. *Organometallics* **1991**, *10*, 3363. (b) Seyferth, D.; Archer, C. M. *Organometallics* **1986**, *5*, 2572.
- (10) Jensen, C. M.; Chen, Y.-J.; Knobler, C. B.; Kaesz, H. D. *New J. Chem.* **1988**, *12*, 649.

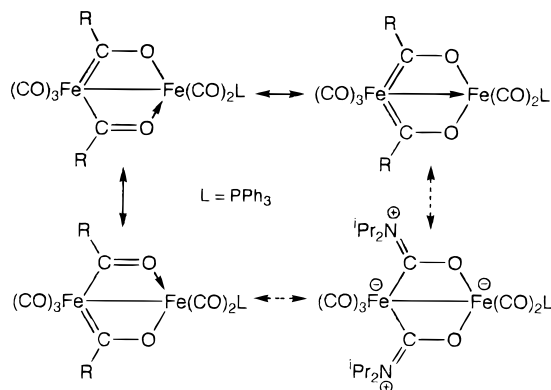
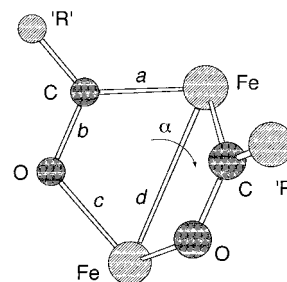


Figure 3. Resonance contributors for the Fe₂(μ-OCR)₂ cores of **1** and **2**.

Table 4. Comparison of the Geometries of the Metallacycles in **1** and **2**



parameter	R = C ₆ H ₃ Me ₂ -2,6 (1)	R = N ⁱ Pr ₂ (2)
a (Å)	1.988(6), 1.954(5)	1.993(3), 2.013(3)
b (Å)	1.243(6), 1.245(6)	1.270(4), 1.274(4)
c (Å)	1.966(4), 1.996(4)	1.977(2), 1.956(2)
d (Å)	2.590(1)	2.569(1)
α (deg)	93	90

The gross molecular structures of **1** and **2** are superficially similar (Figures 1 and 2), comprising two square pyramidal iron centers that are edge-linked back to back *via* the acyl carbonyls. In both structures the iron atoms are displaced out of their basal planes in the direction of their apical substituents [0.15 and 0.15 Å toward phosphorus and 0.27 and 0.28 Å toward the carbonyl ligands in **1** and **2**, respectively]. The edge linking causes the basal planes to be folded by 39 and 36° relative to each other in **1** and **2**, respectively. In **1** the xylyl rings are twisted out of conjugation with the carbonyl bridges (64°), whereas in **2** the trigonal amino groups are in-plane with the carbonyl, leading to noticeable lengthening of both the “C=O” and associated Fe–C bonds but accompanied by a contraction of the Fe–Fe bond relative to **1**. This is consistent with resonance contributors involving a dative Fe–Fe bond. With the exception of the two Fe–C(acyl) bonds in **2** which are essentially identical, there is a marked asymmetry in the pattern of Fe–C and Fe–O bonds within the dimetallacycle destroying the potential C_s symmetry. The reasons for this are not immediately apparent, although in (**1**) there is evidence of an intramolecular hydrogen bond between an ortho phosphine phenyl hydrogen atom and O(15) (H···O, 2.26 Å; C–H···O, 148°) which may contribute to a perturbation in the bonding within the metallabicyclic core.

The two Fe(RCO)₂Fe cores of **1**, **2**, and Fischer's complex may be described by three resonance forms (Figure 3, Table 4), while that in (**2**) may also be described by a fourth contributor involving C=N multiple bonding and a concomitant increase of electron density within the metallabicyclic core. This latter contribution is supported by the molecular stasis revealed by NMR spectroscopy. Each of these requires an Fe–Fe bond

to complete the EAN requirements of each metal in contrast, for example, to the "rhenadiketonates" described by Lukehart which have no apparent direct intermetallic interaction across a planar six-membered bimetallic cycle which approaches planarity.¹¹

Experimental Procedures

General Procedures. All manipulations were carried out under an atmosphere of prepurified dinitrogen using conventional Schlenk-tube techniques. Solvents were purified by distillation from an appropriate drying agent (ethers and paraffins from sodium/potassium alloy with benzophenone as indicator; halocarbons from CaH₂).

¹H, ¹³C{¹H}, and ³¹P{¹H} NMR spectra were recorded on Bruker WH-400 NMR or Jeol JNM EX270 NMR spectrometers and calibrated against internal Me₄Si (¹H), internal CDCl₃ (¹³C), or external H₃PO₄ (³¹P). Infrared spectra were recorded using Perkin-Elmer 1720-X FT-IR or Mattson Research Series 1 spectrometers. FAB Mass spectrometry was carried out with an Autospec Q mass spectrometer using nitrobenzyl alcohol as matrix. Light petroleum refers to that fraction of bp 40–60 °C. All reagents were commercially available and used as received from commercial sources (Aldrich).

Preparation of [Fe₂(μ:σ,σ'-OCC₆H₃Me₂-2,6)₂(CO)₅(PPh₃)] (1). A solution of [Fe(CO)₅] (3.00 g, 15.0 mmol) in diethyl ether (50 mL) was treated with 2,6-dimethylphenyllithium (40 mL, 0.40 mol dm⁻³, prepared from lithium and BrC₆H₃Me₂-2,6) and stirred for 15 min. The mixture was then cooled (dry ice/propanone) and treated with a solution of (CF₃CO)₂O (2.40 mL, 17.0 mmol) in diethyl ether (20 mL). The mixture was stirred at this temperature for 15 min and then treated with triphenylphosphine (6.00 g, 23 mmol) and allowed to warm to room temperature overnight. The yellow precipitate of [Fe(CO)₃-(PPh₃)₂] was removed by decantation and the solvent was removed from the decantate. The oily residue was crystallized from a mixture of dichloromethane and light petroleum to provide the crude product. This was redissolved in dichloromethane and chromatographed (silica gel, -40 °C, CH₂Cl₂ eluant) to provide the desired product. Yield: 0.85 g (7.1%). IR: (CH₂Cl₂): 2037 vs, 1982 vs, 1952 m, 1932 m ν_(CO), 1681 m ν_(RCO) cm⁻¹. IR (Nujol): 2039 vs, 1991 vs, 1972 m, 1952 m, 1930 m ν_(CO), 1641 w ν_(RCO) cm⁻¹. ¹H NMR (CDCl₃, 25 °C): δ 1.88 [s, 12 H, Me], 6.88, 7.06, 7.25, 7.44, 7.61 ppm [m × 5, 18 H, PC₆H₅ and CC₆H₃]. ¹³C NMR: δ 295.7 [d, ³J(PC) = 5.4 Hz, FeCROFe], 218.8 [s, Fe(CO)₂, cis to Fe-Fe], 214.4 [d, ²J(PC) = 5.4 Hz, Fe(CO)₂, cis to P], 209.5 [d, ³J(PC) = 16.1 Hz, FeCO trans to Fe-Fe], 150.1 [C¹(C₆H₅)], 133.9 [d, ²J(PC) = 10.7, C^{2,6}(C₆H₃)], 132.0 [s, C⁴(C₆H₃)], 131.3 [d, ¹J(PC) = 55.3, C¹(C₆H₅)], 128.9 [s, C⁴(C₆H₃)], 128.9sh [C^{3,5}(C₆H₃), not resolved from phosphine peak], 128.4 [d, ³J(PC) = 8.9 Hz], 20.9 ppm [Me] (Note: C^{2,6}(C₆H₃) not identified due to presumed coincidence with phosphine resonances). ³¹P NMR: δ 34.4 ppm. FAB-MS (NBA matrix): m/z = 751 [M - CO]⁺, 641 [M - 5(CO)]⁺.

Preparation of [Fe₂(μ:σ,σ'-OCN¹Pr₂)₂(CO)₅(PPh₃)] (2). A solution of [Fe(CO)₅] (1.00 g, 5.0 mmol) in diethyl ether (30 mL) was treated with lithium diisopropylamide (3.40 mL, 1.50 mol dm⁻³, 5.0 mmol) and then cooled (dry ice/propanone). Mercury(II) chloride (0.69 g, 2.50 mmol) was then added and the mixture was stirred for 15 min. The mixture was allowed to warm to -10 °C at which point triphenylphosphine (2.00 g, 7.50 mmol) was added and the mixture was left to warm to room temperature overnight. The resulting orange precipitate was isolated by filtration and extracted with a mixture of dichloromethane and light petroleum (2:1). The combined extracts were filtered through diatomaceous earth (to remove elemental mercury) and

then chromatographed (silica gel, -40 °C, CH₂Cl₂ eluant) to provide the desired product. Yield: 2.67 g (68%). IR (CH₂Cl₂): 2026 vs, 1965 vs, 1918 m, ν_(CO), 1582 ν_(NCO) cm⁻¹. IR (Nujol): 2021 vs, 1956 vs, 1917 m ν_(CO), 1587 ν_(NCO) cm⁻¹. ¹H NMR (CDCl₃, 25 °C): δ 0.78, 1.01, 1.09, 1.11 [d × 4, 24 H, Me, J(HH) = 6.6 Hz], 3.16, 4.73 [h × 2, 4 H, NCH], 7.18–7.65 [m, 15 H, PC₆H₅]. ¹³C NMR: δ 219.4 [s, Fe(CO)₂, cis to Fe-Fe], 218.4 [d, ³J(PC) = 7.1 Hz, NCO], 216.5 [d, ²J(PC) = 5.4 Hz, Fe(CO)₂, cis to P], 210.0 [d, ³J(PC) = 17.8 Hz, FeCO trans to Fe-Fe], 134.0 [d, ²J(PC) = 10.4 Hz, C^{2,6}(C₆H₅)], 129.6 [s, C⁴(C₆H₅)], 128.4 [d, ³J(PC) = 8.8 Hz], 50.9, 47.1 [NCH], 21.2, 21.1, 20.8(×2) ppm [Me]. (Note: C¹(C₆H₅) obscured by other phosphine resonances). ³¹P NMR: δ 36.6 ppm. FAB-MS (NBA matrix): m/z = 714 [M - CO]⁺, 686 [M - 2CO]⁺, 686 [M - 3CO]⁺, 630 [M - 5CO]⁺.

Crystal Structure Determination of [Fe₂(μ:σ,σ'-OCC₆H₃Me₂-2,6)₂(CO)₅(PPh₃)] (1). Orange plates were obtained by slow diffusion of hexane into a solution of the complex in dichloromethane at -40 °C. A crystal of approximate dimensions 0.40 × 0.40 × 0.20 mm was used for the diffraction study. Intensity data were collected in the ω scan mode on a Siemens P4/PC diffractometer using Mo Kα radiation to a maximum 2θ value of 50°. Table 1 provides a summary of the crystal data, data collection, and refinement parameters for 1. The structure was solved by direct methods, and all the non-hydrogen atoms were refined anisotropically using full-matrix least-squares based on F². The methyl hydrogen atoms were located from a ΔF map, optimized, assigned isotropic thermal parameters [U(H) = 1.5U_{eq}(C)], and allowed to ride on their parent carbon. The remaining hydrogen atoms were placed in calculated positions, assigned isotropic thermal parameters [U(H) = 1.2U_{eq}(C)], and allowed to ride on their parent atoms. Computations were carried out using the SHELXTL PC program system (Version 5.03) to give R = 0.062, R_w = 0.059 for 4364 independent, observed reflections [|F_o| > 4σ(|F_o|)] and 460 parameters. Selected bond lengths and angles are given in Table 2.

Crystal Structure Determination of [Fe₂(μ:σ,σ'-OCN¹Pr₂)₂(CO)₅(PPh₃)] (2). Red blocks plates were obtained by slow diffusion of hexane into a solution of the complex in dichloromethane at -40 °C. A crystal of approximate dimensions 0.70 × 0.40 × 0.23 mm was used for the diffraction study. Intensity data were collected in the ω scan mode on a Siemens P4/PC diffractometer using Mo Kα radiation to a maximum 2θ value of 124°. Table 1 provides a summary of the crystal data, data collection, and refinement parameters for 2. The structure was solved by the heavy-atom method, and all the non-hydrogen atoms were refined anisotropically using full-matrix least-squares based on F². The methyl hydrogen atoms were located from a ΔF map, optimized, assigned isotropic thermal parameters [U(H) = 1.5U_{eq}(C)], and allowed to ride on their parent carbon. The remaining hydrogen atoms were placed in calculated positions, assigned isotropic thermal parameters [U(H) = 1.2U_{eq}(C)], and allowed to ride on their parent atoms. Computations were carried out using the SHELXTL PC program system (Version 5.03) to give R = 0.044, R_w = 0.046 for 5428 independent, observed reflections [|F_o| > 4σ(|F_o|)] and 442 parameters. Selected bond lengths and angles are given in Table 3.

Acknowledgment. We thank the Engineering and Physical Sciences Research Council (U.K.) for a studentship (to S.A.) and the provision of diffractometer and the Leverhulme Trust and the Royal Society for the award of a Senior Research Fellowship (to A.F.H.).

Supporting Information Available: For 1 and 2, tables giving details of the crystallographic data collection, full sets of bond lengths and angles, anisotropic displacement coefficients, H-atom coordinates, and displacement coefficients (16 pages). Ordering information is given on any current masthead page.

(11) (a) Lukehart, C. M. *Acc. Chem. Res.* **1981**, *14*, 109; *Adv. Organomet. Chem.* **1986**, *25*, 45. (b) Lippmann, E.; Robl, C.; Berke, H.; Kaesz, H. D.; Beck, W. *Chem. Ber.* **1993**, *126*, 933.